Monitoring of hydrological hillslope processes via time-lapse ground-penetrating radar guided waves

G. Cassiani[1], C. Strobbia[2], M. Giustiniani[3], N. Fusi[1], G.B. Crosta[1] and P. Frattini[1]

[1] *Dipartimento di Scienze Geologiche e Geotecnologie, Università Bicocca, Milano, Italy*
[2] *European Centre for Training and Research in Earthquake Engineering, Pavia, Italy*
[3] *Dipartimento di Ingegneria Civile, Sezione Georisorse e Ambiente, Università di Trieste, Italy*

(Received March 23, 2005; accepted June 21, 2005)

ABSTRACT Hydrological and hydrogeological dynamics along mountain slopes control many important phenomena, such as shallow landslide triggering and flood generation. The governing factors include: soil thickness, slope and bedrock morphology, rainfall pattern and subsurface groundwater conditions, both in the vadose zone and under the water table. We present the results of a monitoring project undertaken on a large slope parcel in the Alpine region of northern Italy. Both direct (piezometers, tensiometers, etc.) and indirect (geophysical) methods have been used to characterize slope and bedrock morphology as well as changes in soil moisture content over time. In this note, we focus on the use of the ground-penetrating radar (GPR) in surface-to-surface configuration. Recently, the use of multi- and single-offset GPR has been advocated for intermediate scale monitoring of moisture content changes in agricultural soils, e.g. in vineyards. We investigate the applicability of similar techniques to hillslopes. The monitoring has been performed using a PulseEkko 100 radar system. The estimation of the soil moisture content is based on the differential arrival time of direct waves through the air and the soil itself. GPR data can also provide information about the bedrock morphology, with special regard to the degree of fracturing. Care must be taken in data interpretation, because the GPR signal propagates in the soil layer as a guided wave, having a dispersive character (phase velocity is function of frequency) and possibly different modes. Consequently, the wave's first arrival at a different offset cannot be simply interpreted as a direct wave through the shallow soil layer. Inversion of the dispersion curve – phase velocity versus frequency – must be performed to yield velocity and thickness of the soil layer as well as velocity of the bedrock. We show that GPR data, properly processed and inverted, carry significant information about the site structure and hydrological dynamics of mountain slopes.

1. Introduction

The characterization of the shallow subsurface for environmental purposes has been the focus of intense research over the past thirty years. Environmental risks such as those deriving from landslides, floods and soil or groundwater pollution have been increasingly perceived as non-acceptable, driving the need for a better understanding of the physical, hydrological and geological processes controlling such phenomena. In particular, extensive efforts have been expended for the understanding of hydrogeological processes, that ultimately control all subsurface processes having an environmental impact (Anderson and Richards, 1987; Fetter, 1998; Beven, 2001).

Traditional methods for the hydrogeological characterization of the shallow subsurface include borehole drilling, often in conjunction with hydraulic testing, and soil/groundwater sampling and lab analysis. The parameters of interest are natural moisture content, pressure-saturation curves, and hydraulic conductivity. These direct, invasive techniques have several shortcomings, particularly in the unsaturated zone where the sampling procedure disturbs the natural water content, and pressure (suction) measurements are difficult below a few tens of centimetres from the ground surface. In addition, invasive methods can be applied only to a limited number of points in space, and are generally labour-intensive.

For these reasons, the use of non-invasive techniques has found increasing acceptance as a source of data that are complementary to invasive methods. Probably the best established methodology, to be broadly classified as non invasive, is the Time Domain Reflectometry (TDR: Topp *et al*., 1980, 2003; Topp and Davis, 1985). The TDR has been considered a standard method to determine in-situ soil moisture content, in environmental and agricultural science, for over twenty years. The TDR is based on the measurement of travel time, and consequently velocity v, of a fast-rise electromagnetic wave in a waveguide of known length, generally made of two or more metallic prongs that are pushed into the soil. The adopted electromagnetic signal is in the microwave frequency range. The relative permittivity, or bulk dielectric constant κ, is derived from the measured velocity v using:

$$\sqrt{\kappa} = \frac{c}{v} \tag{1}$$

where c is the electromagnetic wave velocity in air ($\simeq$ 0.3 m/ns). The dielectric properties of a partially saturated porous medium are strongly linked to its moisture content, due to the high relative permittivity of water ($\kappa \simeq 81$) as compared with other soil constituents (2 to 4). This fact makes TDR-based determination of soil water content very accurate. The link between the moisture content and the dielectric constant has been the subject of research for over two decades and several empirical and semi-empirical models are available for the conversion (Topp *et al*., 1980; Roth *et al*., 1990; Knoll and Knight, 1994).

The increasing availability of reliable and affordable ground-penetrating radar (GPR) equipment for subsurface exploration (e.g. Davis and Annan, 1989), and the physical similarity between GPR and TDR, have prompted the introduction of moisture content estimation based on GPR measurements (e.g., Hubbard *et al*., 1997; Eppstein and Dougherty, 1998; Alumbaugh *et al*., 2000; Binley *et al.*, 2001, 2002a, 2002b, 2004; Cassiani *et al*., 2004; Cassiani and Binley, 2005). Excellent reviews are given by Davis and Annan (2002), Huisman and Bouten (2003) and Huisman *et al*. (2003).

In particular, GPR has been used to measure moisture content by measuring the propagation velocity of direct waves through the ground using both transmitter and receiver antennas at the ground surface (Du and Rummel, 1994; Chanzy *et al*., 1996; Van Overmeeren *et al*., 1997; Weiler *et al*., 1998; Huisman *et al*., 2001, 2002a, 2002b; Hubbard *et al*., 2002; Grote *et al*., 2003). This approach has some clear advantages over TDR, particularly: (a) the scale of measurement is larger (about a cubic metre at 100 MHz, less at higher frequencies) and the estimated moisture content is therefore representative of a larger support volume; (b) measurements are fast and totally non invasive; (c) a large area can be covered in a limited time, so that spatial variations of

moisture content can be reliably mapped with no need for (uncertain) interpolation of TDR point measurements. The disadvantages of GPR versus TDR are that (a) the volume effectively sampled is not clearly defined a priori, and (b) care must be taken in identifying the nature of the events in the radargram.

In this paper, we will focus on the estimation of moisture content along mountain slopes. Research in the field of slope stability has shown that the majority of slope failures is caused by the infiltration of rainwater (Sidle and Swanston, 1982; Rulon and Freeze 1985; Johnson and Sitar, 1990; Reid, 1994). The mechanism leading to slope failures is the increase of pore–water pressures when water infiltrates the unsaturated soil. For unsaturated soils, the shear strength consists of an effective cohesion, strength contributions from the normal net stress, and matric suction. When infiltration occurs, the matric suction decreases, and the shear strength of the soil is reduced (Fredlund and Rahardjo, 1993). For saturated soils, it is assumed that the effective shear strength reduces linearly with increasing pore pressure, according to the principles of effective stress.

The effect of water infiltrating on slope stability depends on several other factors that control the hydrogeological processes at the slope scale. These factors can be subdivided into two categories (Wu and Sidle, 1995): (a) quasi-static variables and (b) dynamic variables. Quasi-static variables include soil properties (thickness, physical and mechanical characteristics, macropores), seepage in the bedrock and topography (elevation, slope, areas of convergence and divergence, etc.). These factors contribute to the definition of the susceptibility of the slopes to failure and they control the spatial distribution of the landslides. Dynamic or transitory variables are the degree of saturation (or volumetric water content) of the soil and the cohesion due to the presence of roots and/or to partial saturation. These factors control the triggering of failures along susceptible slopes as a consequence of rainwater infiltration. Dynamic variables can change at different rates and on a different time scale (daily, monthly, seasonal, annual, etc.).

Hence, the assessment of landslide susceptibility and the forecast of slope failures requires a detailed characterisation of the soil profile in terms of both hydrological and geotechnical properties and the geometry of the different soil layers.

The characteristics of a mountain slope make it an interesting problem in terms of GPR direct wave interpretation. A soil layer of variable thickness, lying on top of a low-porosity bedrock, stands a good chance of giving rise to faster GPR energy propagating through the bedrock, and potentially generates a critically refracted wave (Bohidar and Hermance, 2002) that can easily overtake the slow direct wave through the soil and manifest itself as the first arrival. In addition, the low velocity topsoil layer may act as a waveguide, sandwiched between the air above and the fast velocity bedrock below. Such a phenomenon has been observed in permafrost areas, and in the presence of fine sediments lying on top of gravel (e.g. Arcone *et al*., 2003). Therefore, the interpretation of GPR data along hillslopes promises to be a fairly interesting challenge. Given the considerations above, the objectives of this study are:

- to study the applicability of GPR direct-wave techniques to measure moisture content on hillslopes, with particular reference to the possibility that guided waves are present because of the shallow low velocity layer;
- to assess the amount of additional information that can be derived from GPR data collected in the process;

- to compare the results of GPR monitoring with other information on moisture content dynamics and geological structure of the site, assessing the value of GPR data with respect to other sources of information.

2. Field site description

The study area is located on the north-western tip of Como Lake (Lombardy, Italy; Fig. 1). Although geographically belonging to the Pre-Alps, from a structural point of view this area is part of the Alps, lying north of the Insubric Line. The Insubric Line, that in Lombardy coincides mainly with the Valtellina axis, is one of the most important periadriatic lineaments, that divides the southern calcareous Prealps from the metamorphic Alps (Di Paola and Spalla, 2000; Spalla *et al*., 2000) and dislocates the northern end of the three main Italian lakes (Maggiore, Como and Garda), with a right lateral component of movement. Geologically the study area is part of the Pennidic thrust; the outcropping formations can be attributed to the so-called Bellinzona Dascio zone (Montrasio, 1990), constituted by medium grade paragneiss with lenses of amphibolites and serpentines, lying subvertically or steeply dipping northward.

The site we investigated is located in the S. Vincenzo Creek basin, where several deep and shallow landslide phenomena have been observed and are still active. The S. Vincenzo Creek erodes and transports large quantities of material. The basin is characterized by numerous faults, some of which active, that cut the valley both longitudinally and transversally. The valley development seems to be linked to the existence of such discontinuities in the bedrock mass (Fig. 1).

The slope parcel selected for detailed monitoring is located on the left hydrographic slope of the S. Vincenzo Creek basin at an elevation of 1150 m a.s.l. in the municipality of Montemezzo;

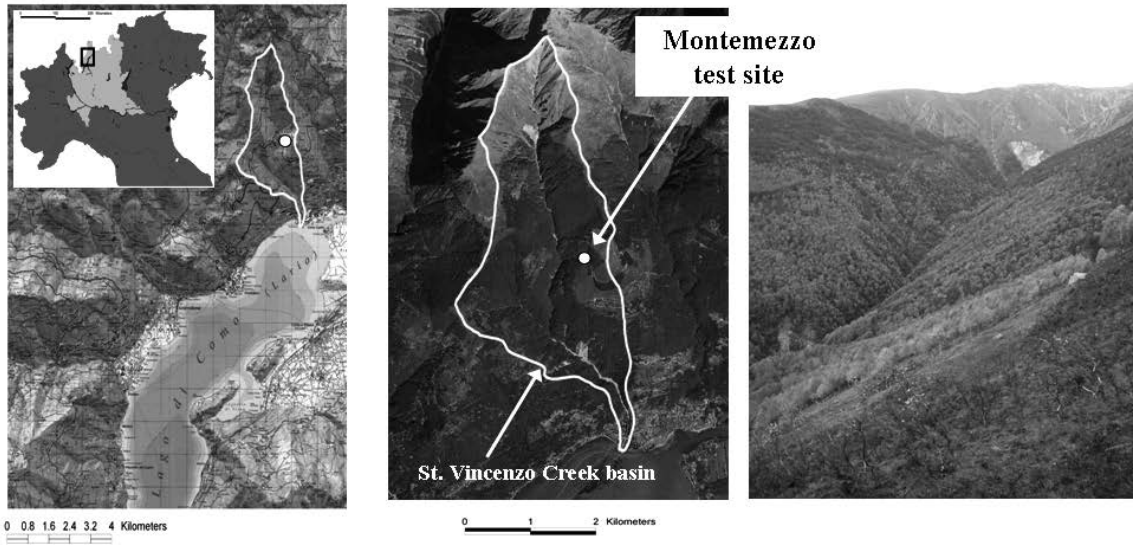

Fig. 1 - Geographical location of the site.

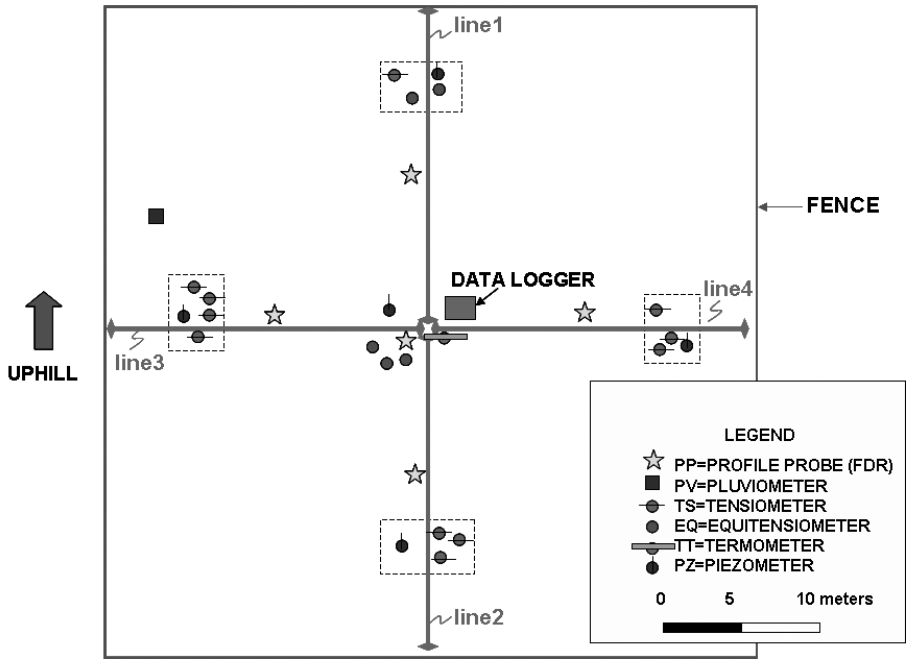

Fig. 2 - Map of the monitored parcel.

it measures about 40 m × 40 m, and faces WSW, with a dip varying between 30° and 40° (Fig. 2). The slope is characterised by extended unconsolidated deposits, with decimetric to metric blocks of different nature (serpentinites, granites, limestones from Valtellina) in a sandy-gravelly matrix, usually interpreted as moraine deposits. In the parcel itself no bedrock outcrops, but a very limited paragneiss outcrop, with subvertical foliation and highly friable, can be seen slightly eastwards of the slope parcel itself. The climatic variability of the slope area under study is due to variations of moisture content caused by (a) the proximity of the lake; (b) the location with respect to the mountain ridge at 2200 m a.s.l. and (c) the presence of strong winds. In winter, the temperature has a strong diurnal variation. The test site is mainly covered with grass, but the surrounding areas are covered with natural forest with beech and birch, and also with natural and imported larch. The soil cover is modelled exclusively by meteoric waters. Infiltration can potentially cause, under very intense rainfall, soil saturation with interflow and possible triggering of shallow landslides in the soil cover and/or partly in the underlying bedrock. Snow cover during winter limits the impact of intense rainfall and prevents the soil from freezing.

The unconsolidated deposits of the parcel have been geomechanically characterized through the following tests: a) in situ: permeability test (Guelph permeameter) and determination of bulk density; b) in laboratory: sieve analysis, determination of specific gravity, residual shear tests. This material, which can be classified according to ASTM as poorly graded sand with gravel, is characterized by medium saturated hydraulic conductivity (of the order of 10^{-6} m/s) and by a friction angle equal to about 35°. The bulk density increases from 650 kg/m^3 at a 0.10 m depth

to 1230 kg/m^3 at a 1.40 m depth, while the specific gravity of the grains increases from 2350 kg/m^3 at 0.20 cm depth to 2650 kg/m^3 at a 1.40 m depth, probably due to the presence of organic matter in the first tens of centimetres.

Hydrological monitoring at the Montemezzo test site is aimed at providing fundamental information necessary for predictive modelling of slope stability, as well as flow and transport phenomena. Monitoring has been performed using both traditional point measurements of moisture content (via dielectric probes - FDR) and hydraulic head (via tensiometers and piezometers), as well as non invasive geophysical techniques, which are the focus of this paper.

3. Radar wave propagation in a thin layer: direct, refracted and guided waves

The measurement of GPR wave velocity in the soil layer is conceptually very simple. The easiest approach consists in measuring the travel time of radar waves between a transmitter antenna, kept at a fixed location, and a receiver antenna that is moved at increasing offset distances. Two events having a distinct linear moveout can be identified on the radargram: the air wave, travelling at 0.3 m/ns, and the direct wave through the ground, travelling at a smaller velocity v (Fig. 3). The ground velocity v is then used in Eq. (1) to derive the soil bulk dielectric constant κ. The estimate of moisture content θ in the soil is then obtained from the bulk dielectric constant using, for instance, the empirical relationship proposed by Topp *et al*. (1980):

$$\theta = (-530 + 292\kappa - 5.5\kappa^2 + 0.043\kappa^3) < 0.0001 \qquad (2)$$

Reflected energy from the bedrock/soil interface, and reflected-refracted energy from the soil/bedrock and the soil/air interface can also be part of the radargram (Fig. 3).

In the case of a thin soil layer resting on the top of a bedrock, as observed at the site of interest, the GPR wavefield can be substantially different from the simple situation above. The propagation velocity in the soil cover is much lower than in the bedrock, primarily because the soil has a much higher porosity than the underlying rock, and can have a much larger moisture content. If, in addition, the thickness of the soil layer is comparable to the dominant wavelength of the GPR energy, the geological structure becomes a refractive waveguide allowing the modal propagation of guided waves, besides the propagation of direct, refracted, reflected, and reflected-refracted waves. The propagation of guided waves, besides carrying further information, can strongly complicate the data and the identification and interpretation of direct and refracted data. The analysis of the guided waves can hence become a need rather than an opportunity: it is therefore crucial to define a model relating the properties of this propagation to the guide parameters (thickness, soil and bedrock velocities; equivalently, the dielectric properties of a medium can be described in its refractive index, defined as $n = c/v$, where c is the speed of light in a vacuum, and v is the speed of light in the medium).

The simplest model that can describe this physical system is an asymmetric slab waveguide, with two infinite parallel planes that define the interfaces between a core of a refractive index n_1 and two cladding layers (the air and the bedrock) with lower refractive indexes n_2 and n_3; the

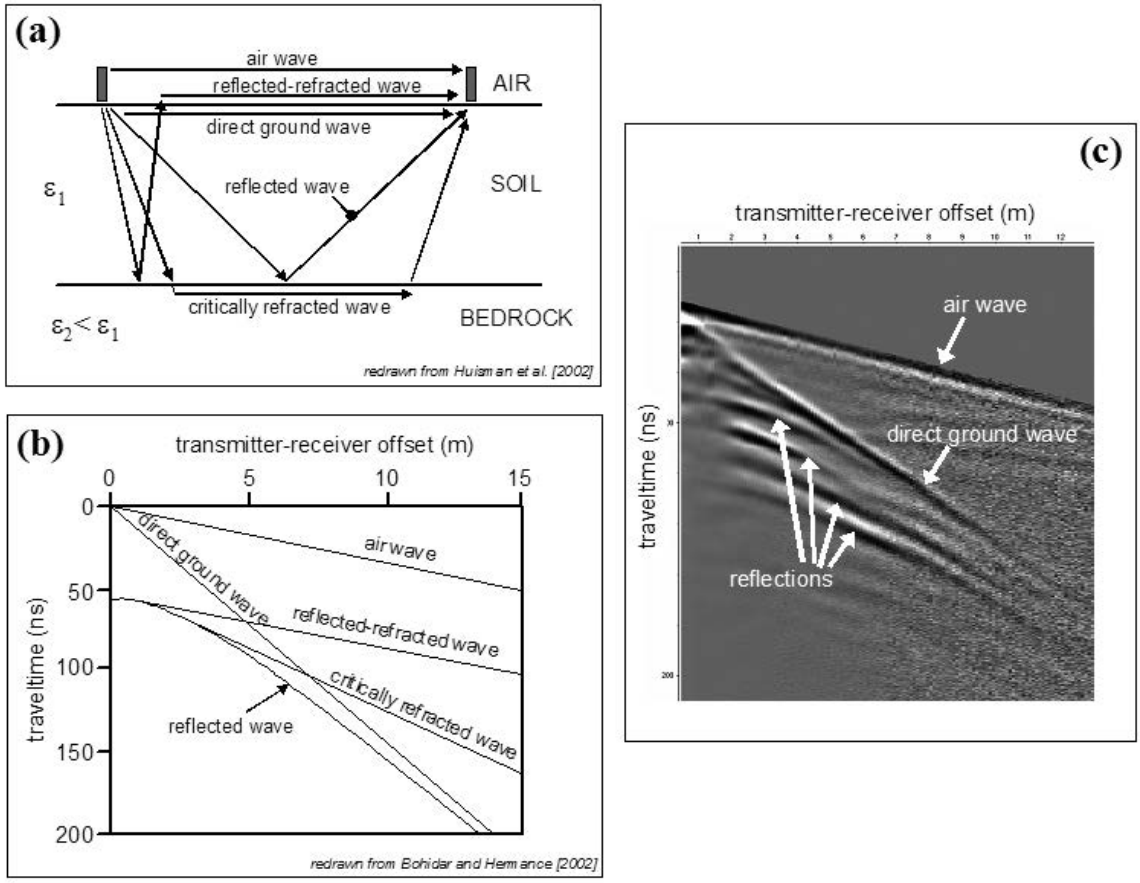

Fig. 3 - Expected GPR wave propagation pathways in surface-to-surface configuration (a); corresponding time-offset relationships (b); example field data (c): Grugliasco (Turin), acquisition with 200 MHz antennas – March 19, 2004 – note the absence of critically refracted events: no bedrock is present.

difference between n_2 and n_3 makes the guide asymmetric. The deployment of antennae (electrical dipoles) parallel to each other justify the assumption of propagation of s-polarised (TE) waves, in which the electric field is perpendicular to the direction of propagation everywhere (Fig. 4).

The guiding effect is due to the presence of a low velocity layer embedded between higher velocity half spaces, allowing the total internal reflection within the waveguide: the energy radiated into the low velocity layer that reaches the lower boundary with an angle greater than the corresponding critical angle (according to Snell's law of refraction) is totally reflected, and reaches the upper boundary where it is again totally reflected. The upper critical angle is always smaller.

The multiple, total internal reflection produces waves inside the low velocity layer that propagate only in the horizontal direction, and evanescent waves outside: because there is no radiation in the bedrock and in the air (even if the fields are not zero) the geometric component

of the attenuation is strongly reduced. The structure is hence able to propagate electro-magnetic waves in the core, and the properties of the propagation depends on the thickness of the guide and on the properties of the different materials.

To find the propagation properties, with the assumed geometry and polarization (Fig. 4), of these waves it is possible to simplify the vector equation of the electric field to read:

$$\frac{\partial^2 E_y}{\partial x^2} + \frac{\partial^2 E_y}{\partial z^2} - \mu_0 \varepsilon \frac{\partial^2 E_y}{\partial t^2} = 0 \tag{3}$$

where E_y is the transversal component of the electric field, x is the axis along the slope direction, z is perpendicular to x (Fig. 4). Considering the x variation of the field first, we can consider the propagation of a harmonic component in the form

$$E_y(x,t) = Ae^{i(k_x x - \omega t)} \tag{4}$$

where k_x is the wavenumber in the x direction.

Consequently, the PDE in Eq. (3) reduces to

$$\frac{\partial^2 E_y}{\partial z^2} - E_y \cdot \left(k_x^2 - \mu_0 \varepsilon \omega^2\right) = 0 \tag{5}$$

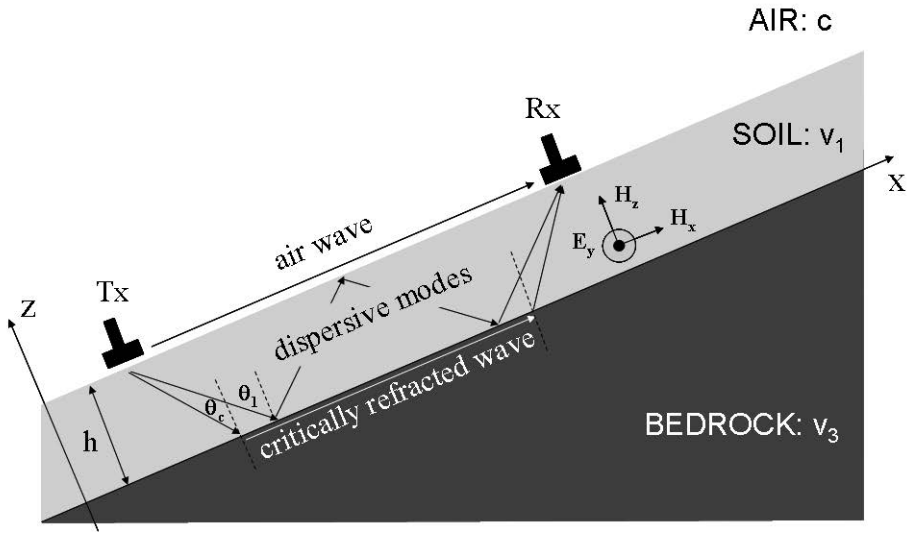

Fig. 4 - Scheme of the slope with radar propagation pathways in the thin waveguide.

Considering now, the variation of the field in the z direction, we can seek a solution in the region of the slab of thickness h, $-h/2<z<+h/2$, in the form

$$E_y(z) = B\cos(\alpha_1 z + \psi) \text{ with } \alpha_1^2 = \left(\mu_0 \varepsilon_1 \omega^2 - k_x^2\right) \tag{6}$$

being ψ a phase shift that accounts for the asymmetry of the slab.

Outside the slab, under the condition of total reflection, the solution is that of an evanescent field, and the solutions are exponentially a decaying function.

$$E_y(z > h/2) = Ce^{-\alpha_2 z} \text{ with } \alpha_2^2 = \left(k_x^2 - \mu_0 \varepsilon_2 \omega^2\right) \tag{7}$$

$$E_y(z < -h/2) = De^{\alpha_3 z} \text{ with } \alpha_3^2 = \left(k_x^2 - \mu_0 \varepsilon_3 \omega^2\right) \tag{8}$$

The constants B, C, D and ψ are determined by imposing the appropriate boundary conditions: the tangential component of the electric field must be of equal amplitude and phase on either side of the interfaces, and the field gradients ($\partial E_y / \partial z$) must also be the same. In order to satisfy these conditions, an eigenvalue equation for TE modes is derived (Budden, 1961):

$$\alpha_1 h = \tan^{-1}(\alpha_2 / \alpha_1) + \tan^{-1}(\alpha_3 / \alpha_1) + m\pi \tag{9}$$

the solutions of which, for a given thickness h and the three refractive indices, describe the properties of the propagating waves. Since $\alpha_i = (\mu_0 \varepsilon_i \omega^2 - k_x^2)$ the above equation relates the frequency $\omega = 2\pi f$ to the horizontal wavenumber k_x, which is the propagation constant, i.e. Eq. (9) implicitly defines the dispersion relation (velocity versus frequency) for the guided waves. Note that different modes of propagation are possible because of the term $m\pi$.

A normalised formulation is given by Kogelnik and Ramaswamy (1974). Defining the dimensionless frequency v as

$$v = k_o \cdot h\sqrt{n_1^2 - n_2^2} = (2\pi \cdot f / c) \cdot h\sqrt{n_1^2 - n_2^2} \tag{10}$$

a dimensionless propagation parameter b as

$$b = \left(n_{eff}^2 - n_2^2\right) / \left(n_1^2 - n_2^2\right) \tag{11}$$

where n_{eff} is the effective horizontal refractive index defined as $n_{eff} = k_x/k_0$, being k_0 the wavenumber in vacuum, and a dimensionless asymmetry parameter a as

$$a = \left(n_2^2 - n_3^2\right) / \left(n_1^2 - n_2^2\right) \tag{12}$$

the eigenvalue equation becomes

$$\nu\sqrt{1-b} = m\pi + \tan^{-1}\sqrt{\frac{b}{1-b}} + \tan^{-1}\sqrt{\frac{b+a}{1-b}} \tag{13}$$

The above equation relates implicitly the frequency f to the wavenumber k_x: given a frequency, the different solutions, corresponding to the different possible modes, can be found searching the zeros Eq. (13).

The solution expresses the dependence of the velocity upon the frequency for the propagation of the guided wave in this system: this implies the existence of a phase velocity, ranging from the intrinsic speed of the low velocity core to the intrinsic speed of the high velocity bedrock.

The most important is the fundamental mode, which dominates the propagation carrying the largest part of energy: Fig. 5 depicts the dispersion curve of the first mode for the asymmetric waveguide and the modal curves of higher modes (1 m at 0.1 m/ns, bedrock at 0.15 m/ns). The low velocity limit is reached asymptotically at high frequency, when the wavelength is small compared to the thickness, while the high velocity limit is approached at low frequency and by higher modes at their cutoff frequency.

Note that, as easily explained by intuition, the core influences the high frequency band, while the bedrock controls the low frequency. The thickness controls the transition between the two velocities.

The guiding effect is stronger for a range of wavelength depending on the thickness, and stronger for stronger velocity contrasts. Moreover, guided normal modes exist only above a cut-off frequency: in an asymmetric waveguide also the fundamental mode has a cut-off frequency, the normalized expression of which is

$$\nu_0 = \tan^{-1}\sqrt{a} \tag{14}$$

In the case presented above (depicted in Fig. 5a), the cut-off normalized frequency is 0.7217, and the frequency is 15.4 MHz: below this value no guided modes can be propagated.

It is hence possible to estimate the soil properties by inverting the dispersion relation of the guided waves. The simplest scheme that simulates the propagation of guided waves is the single layer scheme described above, that is based on the assumption of homogeneity within the core and the bedrock. If the properties of either medium change significantly e.g with depth, a more complicated forward model should be used.

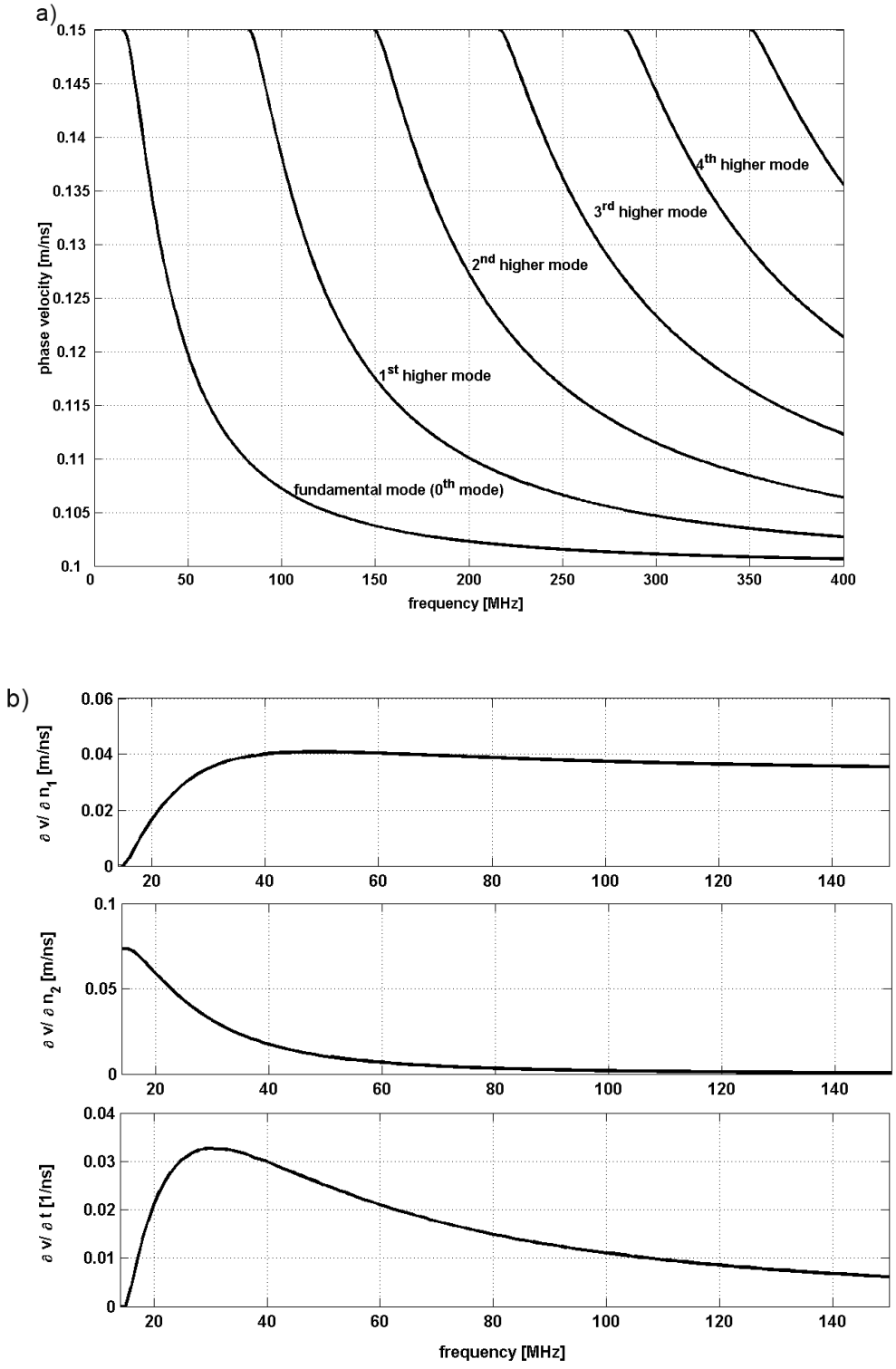

Fig. 5 - Guided wave velocity in a thin waveguide with a 1 m layer at 0.1 m/ns, bedrock at 0.15m/ns. In (a) the modal curves, in (b) the partial derivatives of the fundamental mode phase velocity with respect to the three model parameters.

4. Processing, inversion and interpretation of GPR data

A powerful tool for the identification of the geometric and dielectric properties of the system is the interpretation of the phase velocity of guided waves. When the propagated wavelengths are similar in size to the thickness of the structure, these waves carry most of the energy and are strongly dispersive. These are the characteristics of the GPR walkaway profiles recorded at the Montemezzo site (Figs. 6 and 7). Note the pronounced difference between these records and the corresponding radargrams in a system that manifests no waveguide phenomena (Fig. 3).

The analysis of the dispersion can be performed using different approaches: a very robust technique is based on the wavefield transformation widely adopted in seismic processing to separate and filter events having different apparent velocities, and in the surface wave methods to infer the dispersion characteristics of Rayleigh waves (Strobbia, 2003). The data are transformed from the time-offset domain (t-x) into the frequency-wavenumber (f-k) domain, with a high resolution 2D Fourier transform: the spectral density distribution in the f-k panel allows the identification and separation of the event with different apparent velocity and different frequency. An automatic search algorithm identifies the wavenumber corresponding to the maximum of spectral density at each frequency, and the f-k graphs are easily converted in f-v curves by considering that $v = 2\pi f/k$. The resulting dispersion curve is the final product of the processing phase, and condenses the information contained in the field record (Fig. 8).

The inversion phase takes the dispersion curve and transforms it into estimates of the three governing parameters (thickness, velocity of the soil layer and velocity of the bedrock). Non

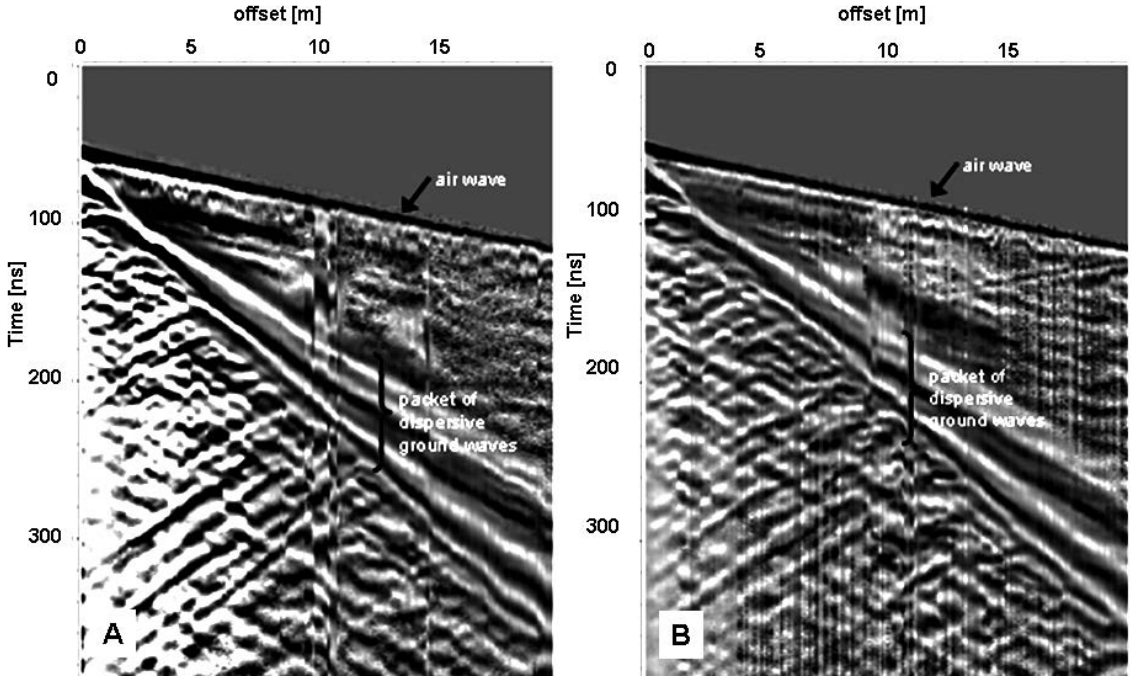

Fig. 6 - WARR1 radargrams at two instants in time over line 1.

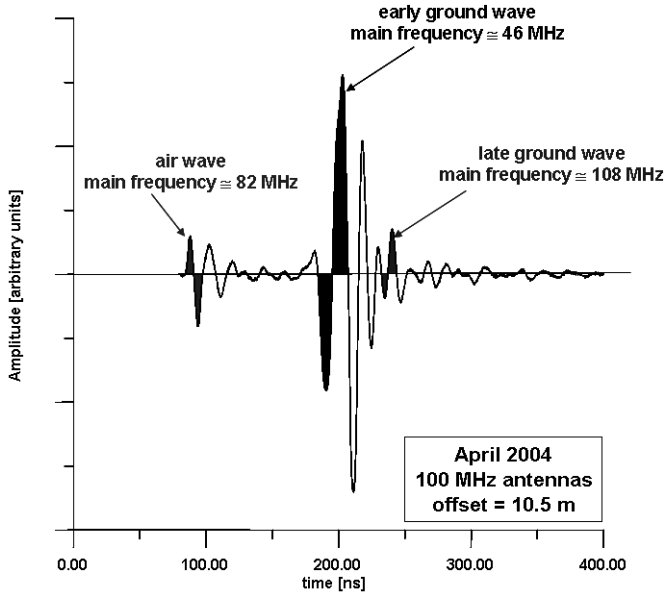

Fig. 7 - Example of trace with dispersive behavior.

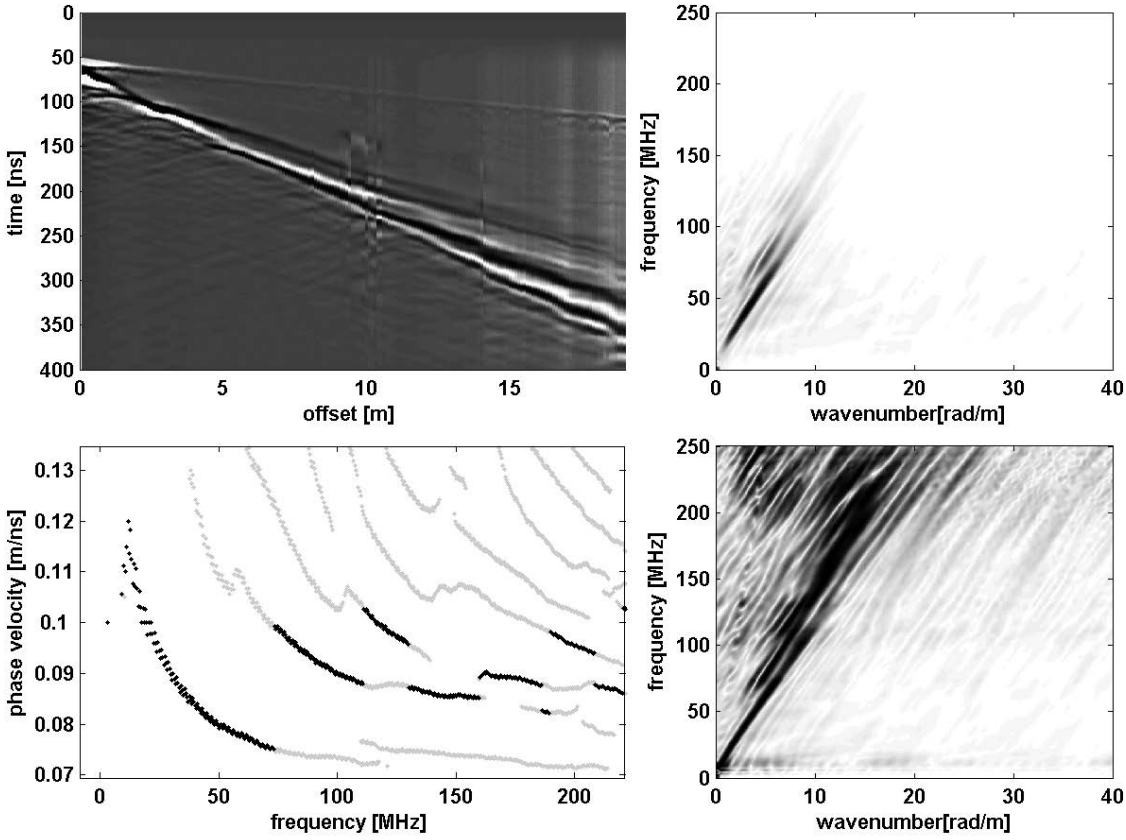

Fig. 8 - Main steps of the processing sequence for guided waves: radargram, f-k spectrum, and dispersion curve.

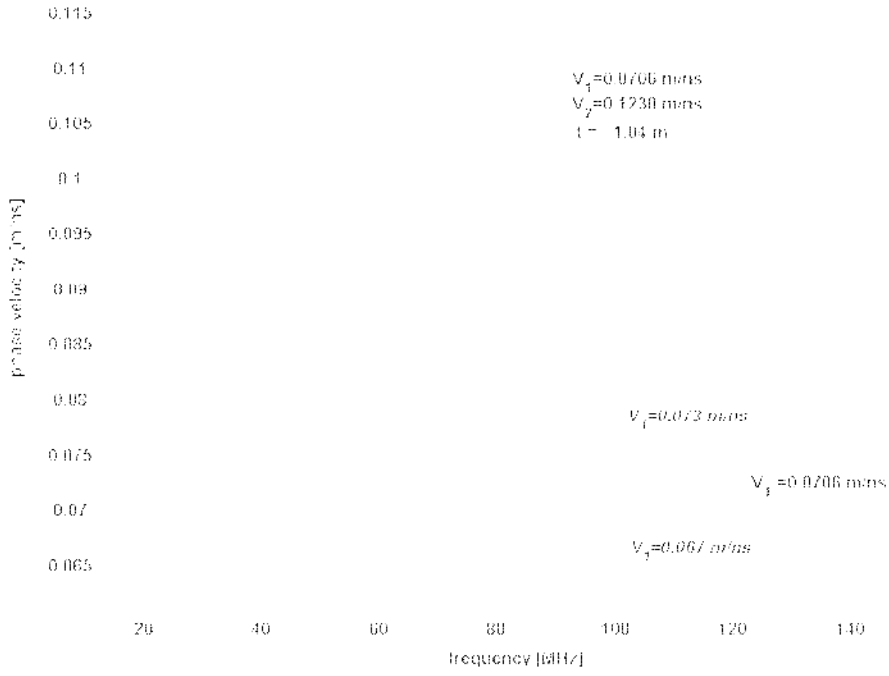

Fig. 9 - Sensitivity of dispersion curves to the guide velocity: the curve of the best-fitting model is shown together with two curves corresponding to the model with a slightly different velocity v_1.

linear least-square fitting is required to match the measured dispersion curve with the results of the forward model described in section 3. The forward model sensitivity to the individual parameters (the refractive indeces n_1 and n_2, and the thickness of the core h) can be assessed by looking at the partial derivatives of the fundamental mode phase velocity (Fig. 5b). The computed dispersion curves are very sensitive to the model parameters (see in particular Fig. 9 for sensitivity to the velocity in the soil layer).

5. Results and discussion

The above processing/inversion procedure has been applied to the data collected at the Montemezzo site from October 2003 to February 2005. We will discuss the results obtained along line 1 (Fig. 2) in detail. At all dates, the transmitter antenna was located at the centre of the cross, and the receiver antenna was moved uphill at increasing offset distances. 100 MHz antennas were used in all cases, with a sampling interval of 0.2 ns and offset increments equal to 0.10 m over the 20 m line. At each station, the signal was stacked 64 times to improve the signal/noise ratio.

The GPR data, analyzed for guided wave dispersion characteristics, provided a picture of the time-evolution of moisture content in the soil and bedrock. The best fit of the field dispersive curves is shown in Fig. 10: the curves are distinctively different at different times, and

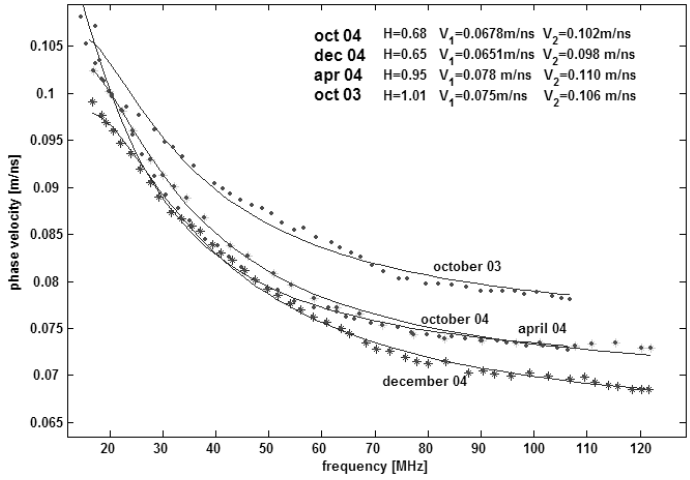

Fig. 10 - Dispersion curves for GPR guided wave, best-fitting curves, for 4 time steps.

consequently, the corresponding models reported in the legend are different. The Topp *et al*. (1980) relationship was used to convert bulk dielectric constant into moisture content values. Note that the use of this relationship for the bedrock is potentially subjected to a great uncertainty, since Topp *et al*. (1980) developed their empirical relationship for granular soils, and not fractured rocks. The estimated inversion parameters at five different time instants are listed in Table 1. The estimates of moisture content derived from the guided wave analysis refer to average values over the thickness of the formation and over the total offset utilized for the analysis. Therefore, these data have a much lower resolution than can be provided by field-deployed moisture content probes. However, GPR derived information has some distinct advantages over the data derived from the probes:

(a) reliability of the GPR estimates is much higher than that of the FDR (dielectric) probes used at the site of interest: FDR is strongly and unpredictably affected by local conditions around the probe itself, including the presence of air gaps and cobbles;
(b) the scale of GPR measurements is consistent with the grid size of distributed rainfall-runoff-infiltration models to be used for flood and/or landslide generation prediction.

Table 1 - GPR velocity of soil and bedrock and waveguide thickness as estimated from the inversion of GPR dispersive waves, and the corresponding estimated volumetric moisture content values, according to the Topp *et al.* (1980) relationship.

	V_{soil} (m/ns)	$V_{bedrock}$ (m/ns)	h (m)	θ_{soil} [-]	$\theta_{bedrock}$ [-]
Oct 03	0.075	0.106	1.01	0.29	0.15
Apr 04	0.078	0.11	0.95	0.27	0.14
Oct 04	0.068	0.102	0.68	0.34	0.16
Dec 04	0.065	0.098	0.65	0.36	0.18
Feb 05	0.071	0.111	0.75	0.32	0.13

Note that the variations of moisture content over time, as estimated by GPR data, are relatively modest. Comparison with point measurements from tensiometers reveals that in correspondence to intense rainfall events moisture content increases strongly, to decline back nearly to the original conditions within 1-2 days from the end of precipitation. Unfortunately FDR measurements are not reliable enough to yield quantitative estimates of moisture content, but they confirm the qualitative pattern shown by the tensiometers. GPR surveys have always been run some time after the end of major precipitation events, and consequently show only smooth variations of moisture content due to seasonality. However, these variations are very interesting particularly because of the strong correlation between moisture content variations in the soil and in the bedrock. This seems to confirm that the bedrock is fairly permeable, albeit with fairly small primary porosity. The bedrock permeability must be linked to fracturing.

Variations in moisture content of the bedrock itself, despite the accuracy of Topp *et al*. (1980) relation for the fractured rock, seems to be confirmed indirectly by electrical tomography surveys. Fig. 11 shows the results of two measurements taken on the same line (lines 3-4 in Fig. 2) at two different dates: substantial changes in resistivity take place in the bedrock. While these resistivity changes cannot be reliably converted into moisture content changes in absence of estimates of the relevant parameters of an empirical correlation, such as Archie's law, these images corroborate the hypothesis that the bedrock is strongly fractured and permeable. Future use of ERT at this site will include more frequent time-lapse measurements.

Depth to the soil-bedrock interface is not easily identifiable in terms of GPR reflections, because the direct waves (through air and soil) arrive at the receiver at the same time as the reflections, especially at short offsets. Depth to bedrock has been independently estimated by

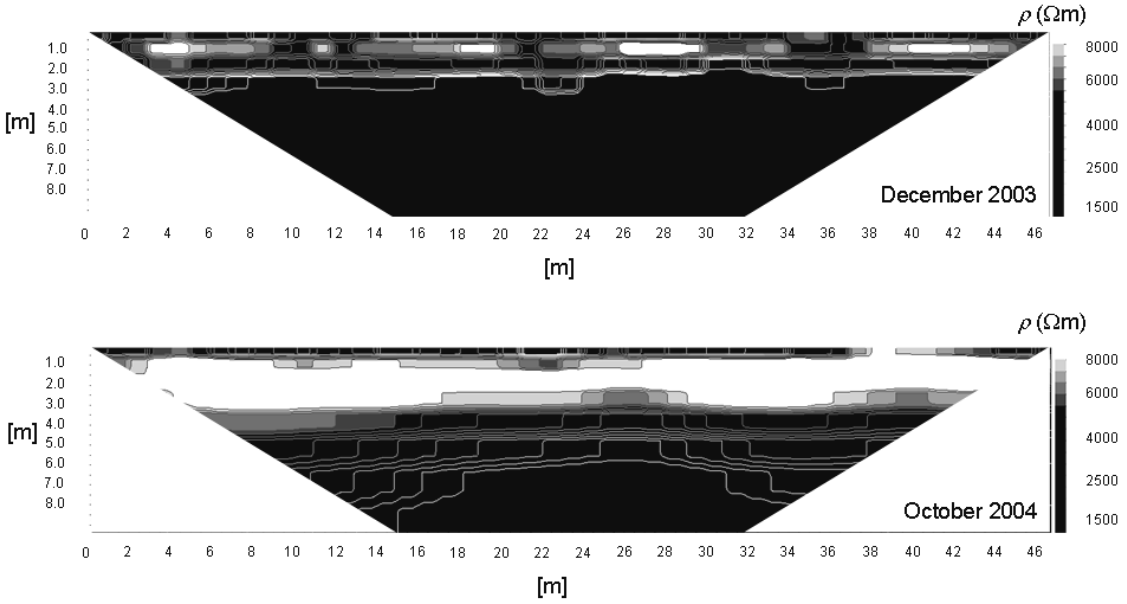

Fig. 11 - Geoelectric data along line 3-4 at two time instants (December 2003, October 2004).

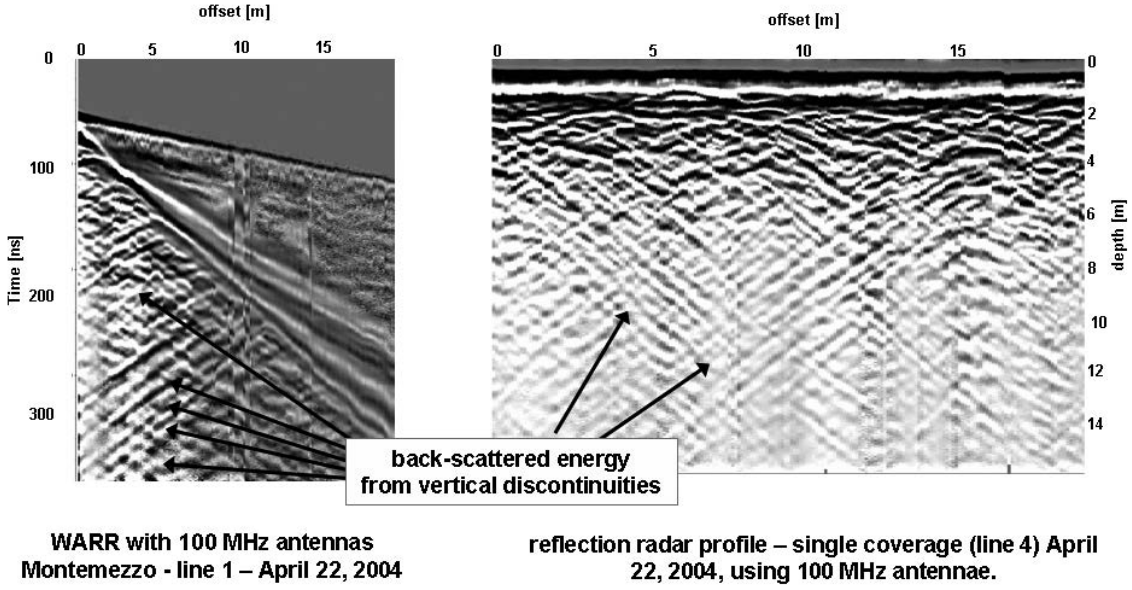

Fig. 12 - Backscattered GPR energy from (sub-)vertical discontinuities in the bedrock. On the left a WARR radargram, on the right a single fold reflection profile.

using seismic refraction and seismic surface wave surveys, that concur to estimate the depth of the soil cover, at the centre of the monitored parcel, around 1.1 m. The soil thickness is visibly smaller a few tens of metres uphill from the monitored site, where parts of the bedrock outcrops locally. Consequently, the estimates of soil thickness derived from GPR guided waves along line 1 (Table 1) are consistent with other observations. In addition, a clear reflected-refracted event in the GPR records (Fig. 6), together with estimates of soil velocity, confirms that the depth to the bedrock is of the order of 1 m. One point to clarify is the changes of soil thickness (ranging from 0.65 m to 1.1 m: Table 1) estimated by GPR guided wave inversion. Note that the forward model described in section 3 assumes that there is a single low-velocity layer sandwiched between two high velocity sub-spaces. This may not be exactly the case at the Montemezzo site, especially in situations when part of the bedrock drains, giving rise to a higher velocity layer in the upper part of the bedrock, below the soil layer itself. Evidence from the electrical resistivity data seems to confirm that this may happen. We believe that the changes in estimated soil thickness over time are likely to be the consequence of using a simplified one-layer forward model in a more complex reality.

The fractured nature of the bedrock is also confirmed by the variable offset and constant offset GPR profiles (Fig. 12): substantial backscattered energy travels horizontally with a velocity close to the bedrock velocity. The reflection profiles confirm the presence of discontinuity in the form of diffraction hyperbolae. This evidence confirms that the bedrock is broken into blocks, both longitudinally and transversally to the slope.

6. Conclusions

In this study, we analyzed the use of surface-to-surface variable offset GPR to measure moisture content changes along mountain slopes. The presence of the underlying low-porosity bedrock changes substantially the nature of the GPR energy transmitted through the ground: the soil layer acts as the core of an asymmetric waveguide, sandwiched between the high-velocity air and the bedrock. Dispersive modes propagate within the layer, and the dispersion curve can be inverted to yield estimates of soil and bedrock velocity, and layer thickness. While conceptually more complex than a simple interpretation of GPR velocity through the soil, in absence of waveguide phenomena, this procedure is still capable of yielding the same information that can be then translated in hydrogeological terms, and particularly in moisture content variations. The presence of a shallow soil cover on top of bedrock is a standard situation in Alpine regions: hence, we believe that the proposed analysis of guided waves should always be taken into consideration when working in such an environment.

The evidence provided by GPR data at the particular site of interest are corroborated by other geophysical and hydrological information, both in terms of geological (geometric) configuration (depth to bedrock and fracturing) and of dynamic (hydrologic) changes.

Extension of the presented approach to include multiple layers in the waveguide may be necessary due to the changes in moisture content of the bedrock.

Acknowledgements. We wish to thank Alberto Godio (Polytechnic of Turin, Italy) for his help in collecting electrical tomography data. Stefano Ferraris (University of Turin, Italy) is acknowledged for collaboration in collecting the GPR data at Grugliasco (Fig. 3).

REFERENCES

Alumbaugh D., Paprocki L., Brainard J. and Rautman C.; 2000: *Monitoring infiltration within the vadose zone using cross-borehole ground penetrating radar*. In: Proc. Symp. Applications of Geophysics to Engineering and Environmental Problems (SAGEEP2000), Environmental and Engineering Geophysical Society, pp. 273-281.

Anderson M.G., Richards K.S.; 1987: *Slope stability - Geotechnical engineering and geomorphology*. J. Wiley & Sons, NY, 648 pp.

Arcone S.A., Peapples P.R., Liu L.; 2003: *Propagation of a ground-penetrating radar (GPR) pulse in a thin waveguide*. Geophysics, **68**, 1922-1933.

Beven K.J.; 2001: *Rainfall-runoff modelling: the primer*. J. Wiley & Sons, NY, 372 pp.

Binley A., Winship P., Middleton R., Pokar M. and West J.; 2001: *High resolution characterization of vadose zone dynamics using cross-borehole radar*. Water Resour. Res., **37**, 2639-2652.

Binley A., Winship P., West L.J., Pokar M. and Middleton R.; 2002a: *Seasonal variation of moisture content in unsaturated sandstone inferred from borehole radar and resistivity profiles*. J. Hydrol., **267**, 160-172.

Binley A.M., Cassiani G., Middleton R. and Winship P.; 2002b: *Vadose zone flow model parameterisation using cross-borehole radar and resistivity imaging*. J. Hydrol., **267**, 147-159.

Binley A.M., Cassiani G. and Winship P.; 2004: *Characterization of Heterogeneity in Unsaturated Sandstone using Borehole Logs and Cross Borehole Tomography*. In: Bridge J. and Hyndman D.W. (eds), SEPM (Society for Sedimentary Geology) Special Publication No. 80, Aquifer characterization, 176 pp.

Bohidar R.N. and Hermance J.F.; 2002: *The GPR refraction method*. Geophysics, **67**, 1474-1485.

Budden K.G.; 1961: *The Wave-Guide mode theory of wave propagation*. Englewood Cliffs, N.J., Prentice-Hall, 325 pp.

Cassiani G. and Binley A. M.; 2005: *Modeling unsaturated flow in a layered formation under quasi-steady state conditions using geophysical data constraints*, Advances in Water Resources, **28**, 467-477.

Cassiani G., Strobbia C. and Gallotti L.; 2004: *Vertical radar profiles for the characterisation of the deep vadose zone*. Vadose Zone Journal, **3**, 1093-1115.

Chanzy A., Tarussov A., Judge A. and Bonn F.; 1996: *Soil water content determination using digital ground penetrating radar*. Soil Sci. Soc. Am. J., **60**, 1318-1326.

Davis J.L. and Annan A.P.; 1989: *Ground penetrating radar for high-resolution mapping of soil and rock stratigraphy*. Geophys. Prospect., **37**, 531-551.

Davis J.L. and Annan A.P.; 2002: *Ground penetrating radar to measure soil water content*. In: Dane J. and Topp G. (eds), Methods of Soil Analysis, part 4, Physical Methods, Soil Sci. Soc. of Am., Madison, Wis., pp. 446-463.

Di Paola S. and Spalla M.I.; 2000: *Contrasting tectonic records in the pre-Alpine metabasite of the Southern Alps (Lake Como, Italy)*. J. of Geodynamics, **30**, 167-189.

Du S. and Rummel P.; 1994: *Reconnaissance studies of moisture in the subsurface with GPR.* In: van Genuchten M.T., Leij F.J. and Wu L. (eds), Proceedings of the Fifth International Conference on Ground Penetrating Radar, Waterloo Cent. for Groundwater Res., Univ. of Waterloo, Waterloo, Ontario, Canada, pp. 1241-1248.

Eppstein M.J. and Dougherty D.E.; 1998: *Efficient three-dimensional data inversion: Soil characterization and moisture monitoring from cross-well ground-penetrating radar at the Vermont test site*. Water Resour. Res., **34**, 1889-1900.

Fetter C.W.; 1998: *Contaminant hydrogeology*. Pearson US Imports & PHIPEs, 500 pp.

Fredlund G. and Rahardjo H.; 1993: *Soil mechanics for unsaturated soils*. John Wiley & Sons, New York, 560 pp.

Grote K., Hubbard S. and Rubin Y.; 2003: *Field-scale estimation of volumetric water content using GPR ground wave techniques*. Water Resour. Res., **39**, 1321, doi: 10.1029/2003WR002045.

Hubbard S.S., Peterson J.E., Majer E.L., Zawislanski P.T., Williams K.H., Roberts J. and Wobber F.; 1997: *Estimation of permeable pathways and water content using tomographic radar data*. Leading Edge, **16**, 1623-1628.

Hubbard S.S., Grote K. and Rubin Y.; 2002: *Mapping the volumetric soil water content of a California vineyard using high-frequency GPR ground wave data*. Leading Edge, **21**, 552-559.

Huisman J.A. and Bouten W.; 2003: *Accuracy and reproducibility of measuring soil water content with the ground water of ground penetrating radar.* J. Environ. Eng. Geophysics, **8**, 65-73.

Huisman J.A., Sperl C., Bouten W. and Verstraten J.M.; 2001: *Soil water content measurements at different scales: Accuracy of time domain reflectometry and ground-penetrating radar*. J. Hydrol., **245**, 48–58.

Huisman J.A., Snepvangers J.J.J.C., Bouten W. and Heuvelink G.B.M.; 2002a: *Mapping spatial variation of surface soil water content: comparison of ground-penetrating radar and time domain reflectometry*. J. Hydrol., **269**, 194-207.

Huisman J., Weerts A., Heimovaara T. and Bouten W.; 2002b: *Comparison of travel time analysis and inverse modeling for soil water content determination with time domain reflectometry*, Water Resour. Res., **38**,1224

Huisman J.A., Hubbard S.S., Redman J.D. and Annan A.P.; 2003: *Measuring soil water content with ground penetrating radar: a review*. Vadose Zone Journal, **2**, 476-491.

Johnson K.A. and Sitar N.; 1990: *Hydrologic conditions leading to debris-flow initiation*. Canadian Geotechnical Journal, **27**, 789-801.

Knoll M.D. and Knight R.; 1994: *Relationship between dielectric and hydrogeologic properties of sand-clay mixtures*. In: Proc. of the Fifth International Conference on GPR, 12-16 June 1994, Kitchener, Ontario, pp. 45-61.

Kogelnik H. and Ramaswamy V.; 1974: *Scaling rules for thin film optical waveguides*. Applied Optics, **13**, 1857-1862.

Montrasio A.; 1990: *Carta Geologica della Lombardia*, 1:250.000. SGN, Istituto Poligrafico e Zecca dello Stato, Roma, Italy.

Reid M.E.; 1994: *A pore-pressure diffusion model for estimating landslide-inducing rainfall*. The Journal of Geology, **102**, 709-717.

Rulon J.J. and Freeze R.A.; 1985: *Multiple seepage faces on layered slopes and their implications for slope-stability analysis*. Canadian Geotechnical Journal, **22**, 347-356.

Roth K., Schulin R., Fluhler H. and Attinger W.; 1990: *Calibration of time domain reflectometry for water content measurement using a composite dielectric approach*. Water Resour. Res., **26**, 2267-2273.

Sidle R.C. and Swanston D.N.; 1982: *Analysis of a small debris slide in coastal Alaska*. Canadian Geotechnical Journal, **19**, 167-174.

Spalla M.I., Siletto G.B., Di Paola S. and Gosso G.; 2000: *The role of structural and metamorphic memory in the distinction of tectono-metamorphic units: the basement of the Como lake in the Southern Alps*. J. of Geodynamics, **30**, 191-204.

Strobbia C.; 2003: *Surface wave method: acquisition, processing and inversion*. PhD thesis, Politecnico di Torino, 317 pp.

Topp G.C. and Davis J.L.; 1985: *Measurement of soil water content using Time Domain Reflectometry*. Soil Sci. Soc. Am. J., **49**, 19-24.

Topp G.C., Davis J.L. and Annan A.P.; 1980: *Electromagnetic determination of soil water content: measurements in coaxial transmission lines*. Water Resour. Res., **16**, 574-582.

Topp G.C., Davis J.L. and Annan A.P.; 2003: *The early development of TDR for soil measurements*. Vadose Zone Journal, **2**, 492-499.

Van Overmeeren R.A., Sariowan S.V. and Gehrels J.C.; 1997: *Ground penetrating radar for determining volumetric soil water content; results of comparative measurements at two test sites*. J. of Hydrology, **197**, 316-338.

Weiler K.W., Steenhuis T.S., Bull J. and Kung K.-J.S.; 1998: *Comparison of ground penetrating radar and time domain reflectometry as soil water sensors*. Soil Sci. Soc. Am. J., **62**, 1237-1239

Wu W. and Sidle R.C.; 1995: *A distributed slope stability model for steep forested basins*. Water Resources Research, **31**, 2097-2110.

Corresponding author: Claudio Strobbia
EUCENTRE - European Centre for Training and Research on Earthquake Engineering
c/o Università di Pavia, Dip. Mecc. Strutt.
Via Ferrata 1, 27100 Pavia, Italy
phone: +39 0382 516925; fax: +39 0382 529131; e-mail: claudio.strobbia@eucentre.it